Liquid Crystals
Publication details, including instructions for authors and subscription information:
http://www.informaworld.com/smpp/title~content=t713926090

Grain boundaries and stacking faults in a Pm3n cubic mesophase

S. D. Hudson; H. -T. Jung; P. Kewsuwan; V. Percec; W. -D. Cho

Online publication date: 06 August 2010

To cite this Article Hudson, S. D. , Jung, H. -T. , Kewsuwan, P. , Percec, V. and Cho, W. -D.(1999) 'Grain boundaries and stacking faults in a Pm3n cubic mesophase', Liquid Crystals, 26: 10, 1493 — 1499
To link to this Article: DOI: 10.1080/026782999203823
URL: http://dx.doi.org/10.1080/026782999203823

LIQUID CRYSTALS, 1999, VOL. 26, NO. 10, 1493–1499

Grain boundaries and stacking faults in a $Pm\bar{3}n$ cubic mesophase

S. D. HUDSON*, H.-T. JUNG, P. KEWSUWAN, V. PERCEC, W.-D. CHO

Department of Macromolecular Science & Engineering,
Case Western Reserve University, Cleveland, Ohio 44106-7202, USA

(*Received 27 April 1999; accepted 19 May 1999*)

A monodendron that over a broad temperature range self-assembles in quasi-spherical supramolecular aggregates organized on a thermotropic cubic $Pm\bar{3}n$ lattice was examined by TEM. Grain boundaries were found parallel to the (1 0 0) and (3 2 0) planes. In well annealed specimens, in which grain boundaries are rare, two types of stacking fault were numerous, suggesting their relatively low energy. In the original $Pm\bar{3}n$ lattice and in the two stacking fault arrangements, the supramolecular aggregates are distorted to an oblate shape, which is likely to be favoured by a crowded microscopic interface between core and tail moieties. Symmetry and phase selection for the ordered arrangement of amphiphilic molecules is discussed.

1. Introduction

Recently a $Pm\bar{3}n$ cubic mesophase (schematically shown in figure 1) comprising oblate spheroidal assemblies has been identified in a thermotropic supramolecular dendrimer [1, 2]. A $Pm\bar{3}n$ cubic phase was also identified in a simpler (lower molecular weight) thermotropic amphiphile [3]; however, the shape of the assemblies was not determined. Several examples of $Pm\bar{3}n$ cubic phases have been found in lyotropic systems [4–11]. The shapes of the assemblies, or micelles, in these lyotropic phases are still disputed. Structural characterization of this and other cubic phases is of interest, because questions remain concerning the universal principles by which these materials self-organize. In this report, we present the first evidence of grain boundaries and stacking faults in a $Pm\bar{3}n$ cubic mesophase. These defects provide insight into the nature of packing within the phase and point to low energy distortions of the structure that are possible.

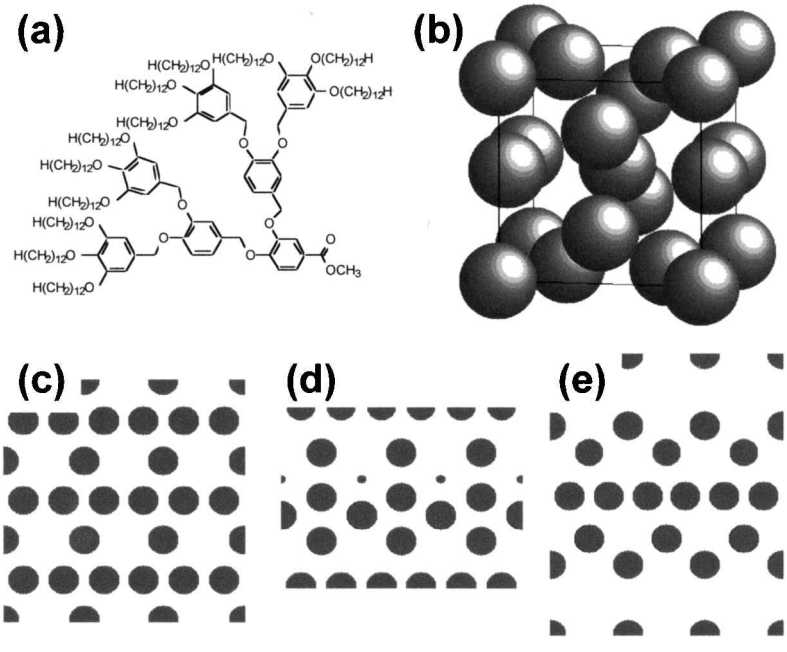

Figure 1. (*a*) Chemical structure of the monodendron; (*b*) schematic representation of the $Pm\bar{3}n$ cubic mesophase comprising quasi-spherical aggregates, or micelles; (*c*) (1 0 0), (*d*) (2 1 0), (*e*) (3 2 0) planes [sections of (*b*)], which may exhibit favourable contact with the amorphous carbon substrate.

*Author for correspondence; e-mail: sdh6@po.cwru.edu

Journal of Liquid Crystals ISSN 0267-8292 print/ISSN 1366-5855 online
http://www.tandf.co.uk/JNLS/lct.htm
http://www.taylorandfrancis.com/JNLS/lct.htm

2. Experimental procedure

We investigated supramolecular assemblies of the dendrimeric compound shown in figure 1(*a*), which self-organizes in a cubic phase at room temperature and disorders sharply to the isotropic phase at 127°C. Ultrathin films of the compound were cast from a dilute methylene chloride solution (0.1 wt %) onto a water surface. After evaporation of the solvent, the film was retrieved on copper grids. The films were coated with a thin layer (~ 10 nm) of evaporated carbon, used for mechanical support during subsequent heat treatment. The films were heated to 130°C and then cooled at a fixed rate (0.1°C min^{-1}) from the isotropic phase to 100°C, before cooling rapidly to 20°C. Films were examined by electron diffraction (ED) before and after staining with RuO_4 (vapours were generated in a closed vessel containing a 0.5 wt % aqueous solution of RuO_4) to determine the conditions that increased image contrast and beam resistance [2], while leaving the symmetry and dimension of the phases unaltered. A 2 min exposure was found to be suitable for this compound. Bright field transmission electron micrographs were obtained using a JEOL 100CX TEM, operated at 100 kV.

3. Results

The compound under investigation forms a $Pm\bar{3}n$ cubic mesophase comprising nearly equivalent, nearly spherical supramolecular assemblies, schematically represented in figure 1(*b*). Upon cooling an ultrathin film of the material from the disordered isotropic melt to the cubic phase, two orientations with respect to the substrate are found. The primary orientation is the [0 0 1] zone, and another less common orientation is the [0 2 3], or possibly the [0 1 2]. The occurrence of these orientations is reasonable considering that they contain planes with a dense packing of micelles in contact with the substrate, as shown in figures 1(*c*, *d*, *e*). These sections of figure 1(*b*) were generated with Rasmol (public domain software); the size of the circles represents the cross-sectional area of each sphere on the selected plane. Therefore the small circles in figure 1(*d*) depict spheres whose centres lie further from the plane. All other circles shown are sectioned nearly along their diameter, and thus are all of similar size. A TEM image of the [0 0 1] projection is shown in figure 2(*a*) (with schematic projection). Images of the other projection have weaker contrast, as expected. For later discussions, we adopt the following convention to illustrate the [0 0 1] projection. Taking the axis out of the plane in figure 2(*a*) to be *z*, we represent the asemblies (or micelles) at $z = 0$, $\frac{1}{4}$, and $\frac{1}{2}$ to be open circles, filled circles and crosses, respectively. The [0 0 1] projection therefore appears as a square array of dots (filled circles) interlaced with rows and columns of circles and crosses. The complete pattern (e.g. along the *y*-axis) involves sequential rows of dots and crosses (A), circles (o), circles and crosses (B), and circles (o), i.e. $(AoBo)_n$. The major defects that we observe consist of stacking faults.

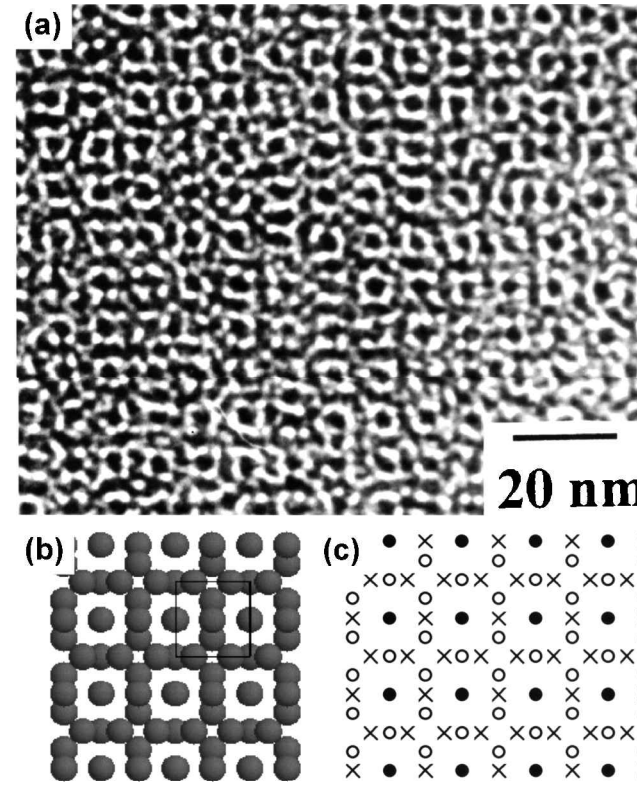

Figure 2. (*a*) TEM micrograph of a [0 0 1] projection of the structure illustrated in figure 1(*b*); (*b*) schematic [0 0 1] projection, in which all the micelles, or aggregates, are represented equally; (*c*) schematic [0 0 1] projection, in which micelles at different levels are illustrated with different symbols, see text.

Diffraction from a single grain yields a single crystal diffraction pattern at low angles. For a grain in which the [0 0 1] zone axis is perpendicular to the film surface, the ED pattern obtained at normal beam incidence contains strong (2 0 0) and (2 1 0) reflections, see figure 3(*a*). Additional low angle reflections are observed: (4 0 0), (3 2 0), (2 2 0) and (3 1 0), listed in order of decreasing intensity. At wide angles, a diffuse ring is observed, centred at 4.6 Å, indicating that the structure at that resolution is disordered. The (2 1 1) reflection, which is strong and of comparable intensity to the (2 0 0) and (2 1 0) reflections, can be observed as expected, if the specimen is tilted ~ 30° or 45° about the [1 0 0] axis, see figures 3(*b*) and 3(*c*), respectively. These patterns represent the [0 $\bar{1}$ 2] and [0 $\bar{1}$ 1] zone axes, respectively. Consistent with predictions, diffraction has also been observed from the [1 1 3], [1 1 2], and [1 1 1] zones.

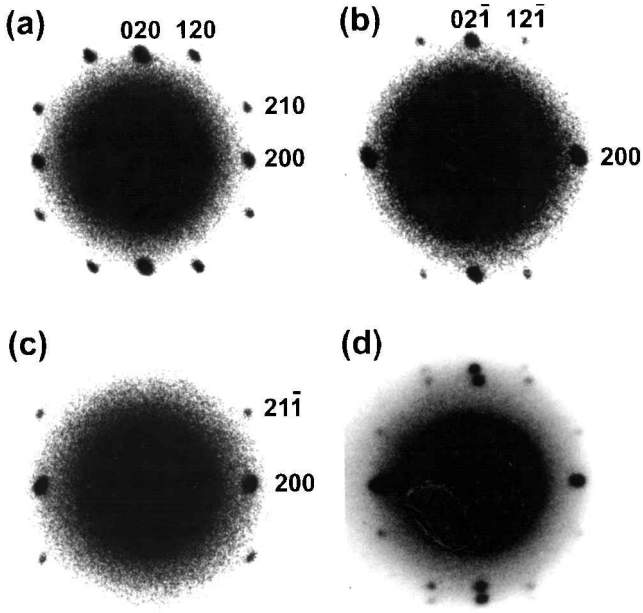

Figure 3. ED of a single grain: (*a*) at normal beam incidence (i.e. the electron beam is normal to the film); (*b*) tilted 27° about the [1 0 0] axis; (*c*) tilted 45° about the [1 0 0] axis; (*d*) ED of a grain boundary for which the two grains are related by a rotation about the [1 0 0] axis, within the plane of the film.

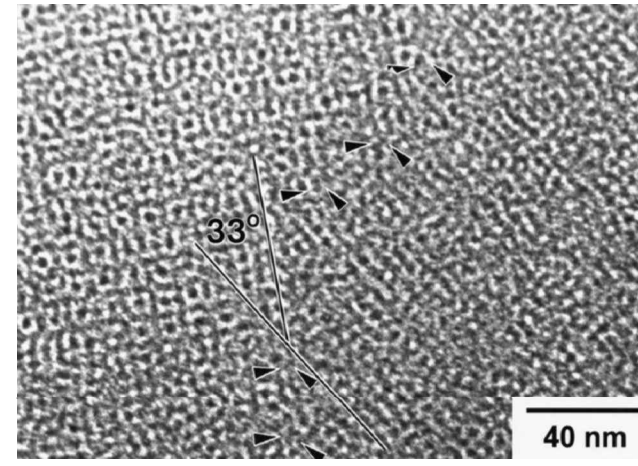

Figure 4. TEM micrograph of a grain boundary for which the two grains are related by a rotation about the [0 0 1] axis, perpendicular to the film. Arrowheads indicate the position of the grain boundary.

Given the two preferred grain orientations with respect the substrate, two types of grain boundary are observed, i.e. the two grains may have either the same or different contact surfaces with the substrate. If they are different, the grain boundary is most easily detected by ED [figure 3(*d*)], because the image contrast is weak, see figure 3(*d*), it is clear that two different crystallographic orientations are present in the region sampled by the selected area aperture, cf. figures 3(*a*) and 3(*b*). These two grains share the same [1 0 0] axis and one is rotated about this axis relative to the other. The pattern therefore appears as a superposition of the diffraction from a single grain taken at two different tilt angles, figures 3(*a*) and 3(*b*).

Alternatively, two grains may share the same (1 0 0) contact plane with the substrate, but be misoriented with respect to one another. Such boundaries may be detected clearly by either diffraction or imaging (figure 4). In this arrangement, the misorientation angle between grains can be measured more accurately and is found to be 33–34°. This angle corresponds to the angle between (1 0 0) and (3 2 0) planes, i.e. 33.7°. Therefore planes as shown in figures 1(*c*) and 1(*e*) are expected to be matched with one another at the grain boundary. In addition, the repeat distances on these two planes are commensurate to within 3%. Consistent with this picture, the grain boundary is not symmetric, but rather lies parallel to the (1 0 0) plane of one of the grains. Specifically, it is apparent in figure 4 that the boundary at the bottom of the image follows the (1 0 0) plane of the grain on the left, whereas as it reaches the upper part of the image, it shifts its direction along the (1 0 0) plane of the grain on the right. Note the similar arrangement of spheres on these two planes.

A number of stacking faults are also present in this material. These are planar defects that do not change the orientation of the grain. Instead, the grains across the fault line are related by a translation. The most easily identified stacking fault involves a translation parallel to the fault interface (figure 5). That is, the grains are slipped with respect to one another. The position of the slip plane, or stacking fault, in figure 5(*b*), using the convention introduced in figure 2(*c*). The pattern at the top of figures 5(*a*) and 5(*b*) is shifted horizontally by half a lattice unit with respect to the pattern at the bottom. In addition to this simple translation, there is also a translation perpendicular to the boundary. Note that, at the boundary, the row containing circles and crosses is arranged in a zig-zag, rather than straight pattern. Instead of the regular packing noted before, $(AoBo)_n$, at the stacking fault, the following sequence is observed: AoBA. In addition to the $a/2$ translation parallel to the fault there is also another translation $a/4$ normal to the fault.

Faults in which the translation is only normal to the fault have also been observed. These are shown schematically in figure 5(*c*), and represent an AoAoBo sequence, i.e. missing layers, Bo, or a translation of $a/2$ normal to the fault. In addition to extended faults, there appear to be many isolated patches where the pattern is disrupted for a few lattice units and then is re-established. One of these faults of limited extent is present in the upper

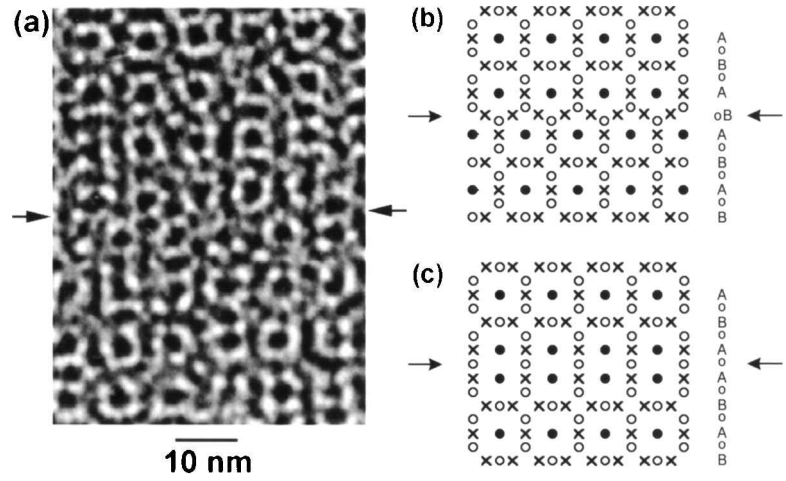

Figure 5. (*a*) TEM micrograph of a stacking fault; (*b*) schematic arrangement of micelles at the fault in (*a*); (*c*) schematic arrangement of another common stacking fault.

centre portion of figure 4. The end of a fault represents a partial dislocation. However, it is difficult to enumerate the stacking faults or the partial dislocations, because in many cases the image is too noisy to distinguish confidently between such a local faulted structure and the perfect structure. One can be more definite where extended faults occur.

4. Discussion

First note that the observed stacking faults are all consistent with a phase comprising quasi-spherical assemblies, and are less consistent with a phase comprising cylinders [1, 2]. In the latter case, each of these boundaries would entail large distortions and even discontinuities of cylinders, representing a significant departure from the equilibrium packing. (Incidentally, these discontinuities would be minimized, but not eliminated, if the tilt grain boundary shown in figure 4 were symmetric or twin. Instead, the observed boundary is asymmetric.) The apparently high number of stacking faults indicates their relatively low energy, as expected from the quasi-spherical model.

The stacking faults also suggest that a variety of packing geometries are of nearly equal energy, that the spheres are deformable and that they interact with one another through a relatively soft pair potential. Figure 5 implies that the degree of distortion of the spheres may not be significantly different from that in the bulk. In both the stacking faults shown in figures 5(*b*) and 5(*c*), the local arrangement of spheres is as depicted in figure 6(*a*). In this structure, one micelle is surrounded by twelve, arranged in two hexagons that are disposed in the same orientation. The $Pm\bar{3}n$ cubic phase has similar layers, yet the setting angle of the hexagons is mutually orthogonal, figure 6(*b*). Figure 6(*b*) represents half of the complete $Pm\bar{3}n$ unit cell, which can be generated by reflecting across a mirror plane, e.g. the

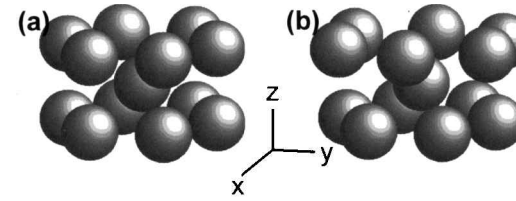

Figure 6. (*a*) Structural motif present at the observed stacking faults; (*b*) similar arrangement found in the $Pm\bar{3}n$ cubic structure.

one containing the upper hexagon, cf. figures 1(*b*), 7(*a*) and 7(*b*). Therefore it seems that a relatively weak distortion of the $Pm\bar{3}n$ structure of this dendrimer involves a change in the setting angle of these hexagons. If the packing in the stacking fault were repeated periodically, $(AoB)_n$ and $(Ao)_n$ structures could be generated, see figures 5(*b*) and 5(*c*), respectively. These represent two different phases that are based on the structural motif illustrated in figure 6(*a*). When this motif is packed on a hexagonal lattice, such that the hexagons share edges, the packing is $(AoB)_n$, and a $P6/mmm$ phase is generated that is similar to the packing of the stacking fault illustrated in figure 5(*b*). When it is packed on an orthorhombic lattice, with axes along x, y, and z, the packing is identical to the $(Ao)_n$ packing illustrated in figure 5(*c*), and a $Pmm2$ phase is generated. These two phases are not observed, i.e. in samples that are annealed slowly enough to yield a sufficiently large number of reflections for structural analysis.

In metal alloys, crystal structure selection depends on the degree of space filling and on the matching of the electronic structure (e.g. bonding) with the lattice site symmetry and coordination number, see e.g. [12]. In the present case, by analogy with the influence of electronic structure in metals, the *shape* of the quasi-spherical assemblies and the softness of their interaction potential

should influence symmetry selection [13]. We will discuss below differences in lattice symmetry, space filling and micelle shape. We will also discuss factors that promote the distortion of micelles as found in the $Pm\bar{3}n$ phase, figure 7(*b*).

Previous experimental studies on phases comprising globular (micellar) supramolecular aggregates have elucidated a total of five different symmetries: $Pm\bar{3}n$ (several examples of small molecule amphiphiles [6, 7, 9] including a computer simulation of short chain non-ionic surfactants in a diluent [14]); $Fd\bar{3}m$ (most commonly observed in systems containing more than one surfactant [15], but also in a single oligomeric diblock surfactant system, $BO_{10}EO_{17}$, where BO denotes butylene oxide and EO denotes ethylene oxide [16]); $P6_3/mmc$ ($C_{12}EO_8$ in water [13], where C denotes an alkyl chain); $Fm\bar{3}m$ (ganglioside lipid in water [8] and polystyrene-*b*-polyisoprene (PS-PI) in hexane [17]); and $Im3m$ (ganglioside in water [8], PS-PI in hexane [17], and diblock copolymer melts [18]). $Fm\bar{3}m$, $Im3m$, and $P6_3/mmc$ are commonly referred to as FCC (face-centered cubic), BCC (body-centered cubic), and HCP (hexagonal 'close packed'), respectively. Although HCP is commonly called close packed, we use quotations to indicate that it is most often only *nearly* close packed. These three have only recently been detected in lyotopic and small molecule systems. A complete *a priori* understanding of the relationship between molecular structure and mesophase symmetry is lacking.

Recent studies on polymeric materials have demonstrated that changing the intersphere potential can change the symmetry of the ordered phase. McConnell and Gast [17] recently studied PS-PI solutions in hexane and found that BCC or FCC spheres were formed depending on the ratio of PS (core) to PI (tail).

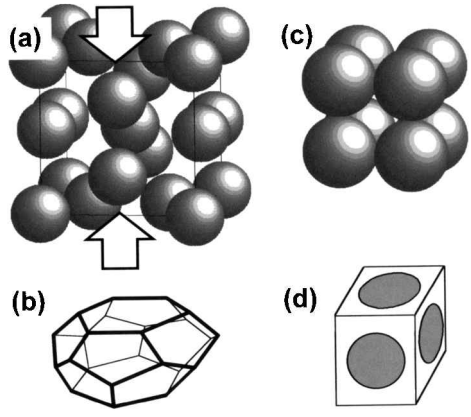

Figure 7. $Pm\bar{3}n$ and simple cubic lattice symmetry and micelle distortion: (*a*) arrows indicate the micelles on the faces of the $Pm\bar{3}n$ unit cell that are distorted; (*b*) the oblate shape of the cavity in which the micelles on the face reside [25]; (*c*) the simple cubic unit cell; (*d*) the cubic cavity of (*c*).

When this ratio is large, the intersphere potential is effectively harder, and FCC packing results. This behaviour is sensible, because the forces that deform polymeric chains are well known, and the relative intersphere potential can be calculated accurately.

However, further work is needed to understand the forces mediated by shorter tails [19–23]. These less understood forces and the distortions of smaller micelles determine the packing of assemblies of small molecules. Many examples of order–order phase transitions have been found also for small molecule surfactant systems. In many cases, however, these systems are complex and contain electrostatic interactions in addition to the shorter range interactions deriving from short chain molecules. Simulation can help by modelling simple systems: lyotropic systems containing a short chain non-ionic surfactant have been studied by Monte Carlo computer simulation [14]. In this study micellar $Pm\bar{3}n$ and $Im3m$ cubic phases were observed, as well as a few non-cubic phases. It is not clear if these latter distorted structures represent other equilibrium structures, or rather are stabilized by finite size effects. The simplest experimental example to date is that of $C_{12}EO_{12}$ studied by Seddon *et al.* [4]. In this case, FCC, BCC, and $Pm\bar{3}n$ spheres are formed as a function of increasing concentration of the amphiphile. Consistent with the hypothesis that we put forward below, the effect of increasing solvent concentration increases the strength of the intersphere potential and leads to phases comprising more spherical, less distorted micelles.

As implied above, the various lattices differ in the *degree* and the *anisotropy* of possible micelle distortion from spherical shape. The *degree* of distortion of a micelle arranged on a particular lattice is related to space filling. If the micelles were hard (undistorted) spheres, each lattice would have a characteristic maximum packing fraction. If the lattice is assembled from deformable spheres, however, then the packing fraction can be higher. Therefore for a given material having a given density, two lattices may be compared by their hard sphere packing fraction, and the lattice with the lower packing fraction must then contain the more deformed spheres. If the hard sphere packing fraction is large, the micelles do not need to be deformed significantly. This hypothesis is similar to an explanation based on the comparison of the pair distribution function for various lattices [24]. (While it is useful to discuss bicontinuous phases in terms of the interfacial curvature and the relative volume fractions of each microdomain, it is more informative to discuss micellar phases in terms of an interparticle potential, because the degree and anisotropy of micelle distortion do not uniquely depend upon the microscopic interfacial curvature. Moreover, there is an ambiguity about how to define the location

of the interface in micellar systems; Luzzati has suggested a concept of variable polar–apolar partition [8].)

Consider the example of a $Pm\bar{3}n$ lattice; its hard sphere packing fraction is 0.524, a value much less than either FCC (0.740) or BCC (0.680). Its micelles are obviously more distorted than those that would be formed by the same material in either FCC or BCC arrangements. Simulations [14], XRD analysis [1], and geometrical analysis [25] agree that the aggregates in a $Pm\bar{3}n$ lattice are oblate and distorted. However, the degree of distortion cannot be the only factor that determines the selection of $Pm\bar{3}n$, because the simple cubic structure, which has a hard sphere packing fraction that is identical to that of $Pm\bar{3}n$, has not been observed. These two phases can be distinguished easily by XRD and no examples of simple cubic have been observed.

Therefore, the symmetry of the aggregate, or micelle, distortion must also be important. The shape of a distorted micelle reflects the shape defined by the neighbours (figure 7). In the case of simple cubic, each sphere would need to deform isotropically, i.e. to become cube shaped. (The deformation in FCC or BCC lattices would also be isotropic: towards a symmetric dodecahedron or symmetric octahedron, respectively.) The deformation required for $Pm\bar{3}n$, however, is directional for most of the spheres, so that the spheres on the cell faces become oblate [1, 14, 25]. An anisotropic packing of micelles, such as in $Pm\bar{3}n$, might occur as a means of reducing some distortions, at the expense of creating others. That is, anisotropic distortion may be created, so as to avoid excessive chain stretching or compression. This exchange is likely to be favourable, when the interface is crowded and the core size is restricted. These conditions apply to familiar examples of the red-blood cell (platelet) or of a deflated rubber ball. Perhaps they also apply to some short amphiphiles. As the tail of an amphiphile becomes shorter, the area that it occupies on the microscopic interface between core and tail becomes correspondingly smaller. For small molecules, with limited extensability, occupying a crowded interface, the micelle is likely to become distorted. If the distortion is anisotropic, it may generate either an oblate, prolate or biaxial shape.

The shape of micelles in isotropic surfactant solutions has been investigated by small angle X-ray scattering analysis assuming uniaxiality [26]. Two systems have been compared. Palmitoyl-lyso-phosphatidyl choline (PLPC) forms isotropic, $Pm\bar{3}n$, and hexagonal columnar phases with increasing surfactant concentrations in water, whereas sodium dodecyl sulphate solutions transform directly from the isotropic to the hexagonal columnar. It was found in both cases that the micelles were prolate, but that in the case of PLPC, the micelles remained much more spheroidal, indicating the avoidance of the cylindrical shape [26].

The anisotropy of micelle, or aggregate, distortion is important for small amphiphiles even when the micelles are quite rigid and nearly spherical, as suggested by the existence of HCP order [13]. As noted above, HCP is an anisotropic packing arrangement that is nearly close packed. Spheres are arranged hexagonally in layers which are stacked in an alternating AB fashion. The repeat distance from one A layer to the next is defined to be c, and the spacing between spheres with the layer as a. There are six neighbours within the layer separated by length a, and six others between layers at a spacing of $a(1/3 + R^2/4)^{1/2}$, where R is the ratio between c and a. When the structure is precisely close packed, $c = a\sqrt{8/3} = 1.633a$, and each sphere has 12 nearest neighbours, separated by a. Therefore when R is near 1.633, this structure then corresponds to rather rigid, nearly isotropic spheres.

The value of R for 38 wt % $C_{12}EO_8$ in water was found to be 1.623, for which the hard sphere packing fraction is 0.736, only slightly less than that for FCC. In this material, therefore, the spheres are quite rigid, being anisotropically distorted only slightly. Therefore, although birefringence is expected in the case of non-cubic symmetry, it was so small, and the micelles so nearly spherical, that none was observed by optical observation between cross polarizers [13]. The shape of the micelles, as defined by their neighbours, depends on the value of R. If R is greater than 1.633, then the micelles are prolate, if less, then oblate. Thus, in the material studied by Clerc [13], the spheres are slightly oblate, having their shortest principal axis along c, i.e. perpendicular to the hexagonal layers. In other words, the intermicelle distance within a hexagonal layer is larger than the intermicelle distance between layers. Anisotropy of micelle distortion, though slight compared with that observed in a $Pm\bar{3}n$ lattice [1, 14], seems to be the key to the existence of the HCP phase, because either BCC or FCC are similarly efficient in terms of hard sphere packing fraction. As mentioned above, short chain amphiphiles may readily adopt an anisometric oblate shape, in order to reduce stretching and compression of chains.

To illustrate the relationship between anisotropic micelle distortion and the selection of HCP over FCC, remember that FCC represents periodic ABC packing of close-packed layers, while HCP represents only periodic AB layers. One phase can be transformed to the other through the periodic placement of stacking faults. These 'faults' can be caused by micelle distortion, because the compression of layers A and B together leads to a crowding of sites C and an opening of sites A next to layer B, and *vice versa*. Thus the alternating AB packing of HCP derives from anisotropic distortions of the micelles.

For HCP, the anisotropy of micelle distortion transfers to an anisotropy of the overall structure. In the case of $Pm\bar{3}n$, however, overall isotropy is maintained, because three pairs of spheres distort along each of three mutually perpendicular directions (only one shown in figure 7). The prevalence of BCC in high molecular weight block copolymers [27, 28] suggests that anisotropy of micelle distortion in that case is not favourable. This seems reasonable in light of the relatively large distance between junction points (~ 5 nm) [29]. Crowding of junction points in small molecule systems is likely to favour anisotropic distortions, as suggested above.

5. Conclusions

TEM analysis of a supramolecular dendrimer that exhibits a $Pm\bar{3}n$ cubic phase has disclosed low energy grain boundaries and stacking faults in well annealed samples. These defects are consistent with the aggregate model developed previously for this phase [1, 2, 25]. Two possible non-equilibrium phases (packing arrangements that have $P6/mmm$ or $Pmm2$ symmetry) are suggested, based upon the structure of the stacking faults. In each of these proposed structures and in the $Pm\bar{3}n$ phase, the majority of quasi-spherical assemblies are distorted anisotropically into an oblate shape. Comparison of these results with others reported in the literature suggest that for quasi-spherical assemblies of amphiphiles, phase selection is influenced by the *degree* and the *anisotropy* of aggregate, or micelle distortion that is required by the phase.

The authors gratefully acknowledge NSF grants DMR-9806684 and DMR-9708581 for support of this work. SDH is also grateful for thoughtful discussions with Prof. R. G. Larson.

References

[1] Balagurusamy, V. S. K., Ungar, G., Percec, V., and Johansson, G., 1997, *J. Am. chem. Soc.*, **119,** 1539.
[2] Hudson, S. D., Jung, H.-T., Percec, V., Cho, W.-D., Johansson, G., Ungar, G., and Balagurusamy, V. S. K., 1997, *Science*, **278,** 449.
[3] Borisch, K., Diele, S., Goring, P., Kresse, H., and Tschierske, C., 1997, *Angew. Chem. int. Ed. Engl.*, **36,** 2087.
[4] Sakya, P., Seddon, J. M., Templer, R. H., Mirkin, R. J., and Tiddy, G. J. T., 1997, *Langmuir*, **13,** 3706.
[5] Cribier, S., Gulik, A., Fellmann, P., Vargas, R., DeVaux, P. F., and Luzzati, V., 1993, *J. mol. Biol.*, **229,** 517.
[6] Delacroix, H., Gulik-Krzywicki, T., Mariani, P., and Luzzati, V., 1993, *J. mol. Biol.*, **229,** 526–539.
[7] Fontell, K., Fox, K. K., and Hanson, E., 1985, *Mol. Cryst. liq. Cryst. Lett.*, **1,** 9.
[8] Gulik, A., Delacroix, H., Kirschner, G., and Luzzati, V., 1995, *J. Phys. II Fr.*, **5,** 445.
[9] Luzzati, V., Vargus, R., Mariani, P., Gulik, A., and Delacroix, H., 1993, *J. mol. Biol.*, **229,** 540.
[10] Vargus, R., Mariani, P., Gulik, A., and Luzzati, V., 1992, *J. mol. Biol.*, **225,** 137.
[11] Alexandridis, P., 1998, *Macromolecules*, **31,** 6935.
[12] Pearson, W. B., 1972, *The Crystal Chemistry and Physics of Metals and Alloys* (New York: Wiley-Interscience).
[13] Clerc, M., 1996, *J. Phys. II Fr.*, **6,** 961.
[14] Larson, R. G., 1994, *Chem. eng. Sci.*, **49,** 2833.
[15] Delacroix, H., Gulik-Krzywicki, T., and Seddon, J. M., 1996, *J. mol. Biol.*, **258,** 88.
[16] Alexandridis, P., Olsson, U., and Lindman, B., 1997, *Langmuir*, **13,** 23.
[17] McConnell, G. A., and Gast, A. P., 1997, *Macromolecules*, **30,** 435.
[18] Koppi, K. A., Tirrell, M., and Bates, F. S., 1994, *J. Rheol.*, **38,** 999.
[19] Helm, C. A., and Israelachvili, J. N., 1993, *Methods Enzymol.*, **220,** 130.
[20] Kong, Y. C., Nicholson, D., Parsonage, N. G., and Thompson, L., 1996, *Mol. Phys.*, **89,** 835.
[21] Manne, S., and Gaub, H. E., 1995, *Science*, **270,** 1480.
[22] Mao, G. Z., Tsao, Y. H., Tirrell, M., Davis, H. T., Hessel, V., Vanesch, J., and Ringsdorf, H., 1994, *Langmuir*, **10,** 4174.
[23] Hillmyer, M. A., Bates, F. S., Almdal, K., Mortensen, K., Ryan, A. J., and Fairclough, J. P. A., 1996, *Science*, **271,** 976.
[24] Larson, R. G., private communication.
[25] Charvolin, J., and Sadoc, J. F., 1988, *J. Phys. Fr.*, **49,** 521.
[26] Castelletto, V., Itri, R., and Amaral, L. Q., 1997, *J. chem. Phys.*, **107,** 638.
[27] Inoue, T., Soen, T., Hashimoto, T., and Kawai, H., 1969, *J. polym. Sci. A2*, **7,** 1283.
[28] Leibler, L., 1980, *Macromolecules*, **13,** 1602.
[29] Hashimoto, T., Tanaka, H., and Hasegawa, H., 1990, *Macromolecules*, **23,** 4378.